Kinetic experiments were carried out with 0.6 M Cp_2ZrMe_2 and 0.23 M $EtAlMe_2$ in neat Me_3Al. Product formation was followed by ^{13}C NMR spectroscopy. The method of Levin and Eberhart[25] was used to calculate second-order rate constants. Integration of the rate equation gave excellent correlation coefficients with $R = 0.998$ at 22 °C and 0.996 at 40 °C. The rate is too fast at 60 °C for accurate measurements, and R decreased to 0.976.

Acknowledgment. We are grateful to members of the 3M Analytical and Properties Research laboratory for physical data and to Prof. J. E. Bercaw and Drs. K. A. Brown-Wensley and F. N. Tebbe for helpful discussions.

---

(25) Levin, E.; Eberhart, J. G. *J. Chem. Educ.* **1989**, *66*, 705.

Preparation, Structure, and Formation Mechanism of *cis*-$RuH(OAr)(PMe_3)_4$ (Ar = C_6H_5, C_6H_4-*p*-Me) and *cis*-$RuH(OC_6H_4$-*p*-$CN)(PMe_3)_4(HOC_6H_4$-*p*-$CN)$

Kohtaro Osakada,* Kimitaka Ohshiro, and Akio Yamamoto*,[†]

Research Laboratory of Resources Utilization, Tokyo Institute of Technology,
4259 Nagatsuta, Midori-ku, Yokohama 227, Japan

Received May 22, 1990

Reactions of $RuH_2(PMe_3)_4$ with phenol, *p*-methylphenol, and *p*-cyanophenol give the hydrido–aryloxido complexes *cis*-$RuH(OPh)(PMe_3)_4$ (1), *cis*-$RuH(OC_6H_4$-*p*-$Me)(PMe_3)_4$ (2), and *cis*-$RuH(OC_6H_4$-*p*-$CN)(PMe_3)_4(HOC_6H_4$-*p*-$CN)$ (3-HOC_6H_4-*p*-CN), respectively. NMR spectra (^1H, ^{13}C, and ^{31}P) of these complexes are consistent with the cis structures. The ^1H NMR spectrum of complex 3-HOC_6H_4-*p*-CN at −40 °C in CD_2Cl_2 shows a signal due to the OH hydrogen of the associated *p*-cyanophenol at 16.3 ppm, indicating the presence of O–H···O hydrogen bonding between the *p*-cyanophenoxide and the *p*-cyanophenol. The molecular structure of 2 has been determined by X-ray crystallography. Crystal data: monoclinic, space group $P2_1/a$, $a = 29.332$ (5) Å, $b = 13.741$ (8) Å, $c = 13.568$ (3) Å, $\beta = 102.37$ (2)°, $V = 5341.9$ Å^3, $Z = 8$, $R = 0.061$, $R_w = 0.070$ for 6011 reflections with $|F_o| > 3\sigma(F_o)$. ^1H and ^{31}P NMR spectra of the reaction mixture of $RuH_2(PMe_3)_4$ with phenol at low temperature indicate formation of an ionic complex formulated as $[RuH_3(PMe_3)_4]OPh$ (4), which is gradually converted into 1 at room temperature. Reaction mixtures of $RuH_2(PMe_3)_4$ with other Brønsted acids such as HBF_4 and 1,1,1,3,3,3-hexafluoro-2-propanol show similar ^1H and $^{31}P\{^1H\}$ NMR signals at low temperature, indicating the formation of complexes such as $[RuH_3(PMe_3)_4]BF_4$ and $[RuH_3(PMe_3)_4]OCH(CF_3)_2$. The ^1H NMR signal of hydrogen bonded to ruthenium in $[RuH_3(PMe_3)_4]OCH(CF_3)_2$ shows a value of 70 ms for T_1 at −40 °C and 500 MHz.

Introduction

Recent studies on late-transition-metal phenoxides with tertiary phosphine ligands have revealed their interesting properties such as C–O bond formation through coupling of the phenoxide and acyl ligands,[1,2] association of the phenoxide ligand with phenol through O–H···O hydrogen bonding,[3-5] and CO insertion into the metal–phenoxide bond.[6] The phenoxide complexes of Pd, Pt, Rh, and Ir were prepared easily by reactions of hydride or alkyl complexes of these metals with phenol. However, similar $\eta^1(O)$-bonded phenoxide complexes with tertiary phosphine ligands have not been separated for ruthenium. Previously the reaction of $RuH_2(PPh_3)_4$ with phenol was reported to liberate two PPh_3 ligands and give a complex formulated as $RuH(\eta^5\text{-}C_6H_5{=}O)(PPh_3)_2$, having an η^5-coordinated phenoxide ligand.[7]

We have investigated the preparation of ruthenium complexes having $\eta^1(O)$-bonded aryloxide ligands by the reaction of $RuH_2(PMe_3)_4$, having nonlabile PMe_3 ligands, with phenols and studied their structures and chemical properties. Several ruthenium aryloxide complexes of the type *cis*-$RuH(OAr)(PMe_3)_4$ and *cis*-$RuH(OAr)(PMe_3)_4(HOAr)$ were isolated and characterized by means of IR and NMR spectroscopy and X-ray crystallography. NMR studies of the reaction mixture of $RuH_2(PMe_3)_4$ with phenol at low temperature revealed the initial formation of the ionic complex $[RuH_3(PMe_3)_4]OPh$, which released dihydrogen to give *cis*-$RuH(OPh)(PMe_3)_4$ at room temperature.

Here we report the preparation, structures, and mechanism of formation of these ruthenium aryloxide complexes.

Results and Discussion

Preparation and Characterization of *cis*-$RuH(OC_6H_5)(PMe_3)_4$ (1) and *cis*-$RuH(OC_6H_4$-*p*-$Me)(PMe_3)_4$ (2). Reactions of $RuH_2(PMe_3)_4$ with a slight excess of phenol and *p*-methylphenol at room temperature

---

[†] Present address: Department of Applied Chemistry, School of Science and Engineering, Waseda University, Ohkubo, Shinjyuku-ku, Tokyo 169, Japan.

(1) Komiya, S.; Akai, Y.; Tanaka, K.; Yamamoto, T.; Yamamoto, A. *Organometallics* **1985**, *4*, 1130.

(2) Bernard, K. A.; Atwood, J. D. *Organometallics* **1989**, *8*, 795.

(3) Kegley, S. E.; Schaverien, C. J.; Freudenberger, J. H.; Bergman, R. G.; Nolan, S. P.; Hoff, C. D. *J. Am. Chem. Soc.* **1987**, *109*, 6563.

(4) (a) Braga, D.; Sabatino, P.; Di Bugno, C.; Leoni, P.; Pasquali, M. *J. Organomet. Chem.* **1987**, *334*, C46. (b) Di Bugno, C.; Pasquali, M.; Leoni, P.; Sabatino, P.; Braga, D. *Inorg. Chem.* **1989**, *28*, 1390.

(5) (a) Kim, Y.-J.; Osakada, K.; Takenaka, A.; Yamamoto, A. *J. Am. Chem. Soc.* **1990**, *112*, 1096. (b) Osakada, K.; Kim, Y.-J.; Yamamoto, A. *J. Organomet. Chem.* **1990**, *382*, 303.

(6) Rees, W. M.; Churchill, M. R.; Fettinger, J. C.; Atwood, J. D. *Organometallics* **1985**, *4*, 2179.

(7) Cole-Hamilton, D. J.; Young, R. J.; Wilkinson, G. *J. Chem. Soc., Dalton Trans.* **1976**, 1995.

0276-7333/91/2310-0404$02.50/0

Table I. NMR Data for Complexes 1–3

	$^1H^a$		$^{13}C\{^1H\}^b$			
complex	$P(CH_3)_3^d$	Ru–*H*	$P(CH_3)_3^e$	aromatic^f	other	$^{31}P\{^1H\}^c$
1	1.4–1.2	–8.0 (dq, 99 and 28 Hz)	27.0 (d, 26 Hz)	171.3 (s)		16.4 (33 and 18 Hz)
			22.6	128.3 (s)		2.0 (33 and 27 Hz)
			20.4 (d, 17 Hz)	120.2 (s)		–11.5 (27 and 18 Hz)
				108.9 (s)		
2	1.4–1.2	–7.9 (dq, 99 and 27 Hz)	26.8 (d, 27 Hz)	168.7 (s)	20.1 (s)^g	15.3 (33 and 17 Hz)
			22.3	128.8 (s)		1.4 (33 and 26 Hz)
			20.0 (d, 17 Hz)	119.5 (s)		–12.6 (26 and 17 Hz)
				116.8 (s)		
3	1.5–1.2	–9.3 (dq, 99 and 27 Hz)	24.5 (d, 27 Hz)	171.2 (s)	126.9 (s)^h	7.4 (38 and 25 Hz)
			22.7	167.6 (s)*	121.3 (s)*	–10.1 (38 and 22 Hz)
			21.2 (d, 17 Hz)	133.8 (s)		–20.4 (25 and 22 Hz)
				133.4 (s)*		
				118.7 (s)		
				117.5 (s)*		
				92.9 (s)		
				96.2 (s)*		

[a] At 100 MHz and –40 °C in CD_2Cl_2. Chemical shifts (δ) were determined by reference to $CHDCl_2$ contained in the solvent at δ 5.32. *J*(PH) values are in parentheses. Abbreviation: dq, doublet of quartets. [b] At 125 MHz and –40 °C in CD_2Cl_2. Chemical shifts are given in ppm from the center of the signals due to CD_2Cl_2 (53.8 ppm). Abbreviations: s, singlet; d, doublet. *J*(CP) values are in parentheses. [c] At 40 MHz and –40 °C in CD_2Cl_2. Chemical shifts are given in ppm from external 85% H_3PO_4. All the complexes show A_2MX patterns (see text). *J*(PP) values are in parentheses. [d] Detailed coupling patterns were not clarified due to overlapping of the signals with each other. [e] Signals at 22.6, 22.3, and 22.7 ppm for complexes 1–3 are observed as triplets due to virtual coupling (observed splitting of 13 Hz) and assigned to those of two PMe_3 ligands situated at mutually trans positions. [f] Assigned to ipso, meta, ortho, and para carbons, respectively, from low to high field. Signals with asterisks are due to the associated *p*-cyanophenol. [g] C_6H_4–CH_3. [h] CN. Signals marked with asterisks are due to the associated *p*-cyanophenol.

give the complexes *cis*-$RuH(OC_6H_5)(PMe_3)_4$ (1) and *cis*-$RuH(OC_6H_4\text{-}p\text{-}Me)(PMe_3)_4$ (2), respectively.

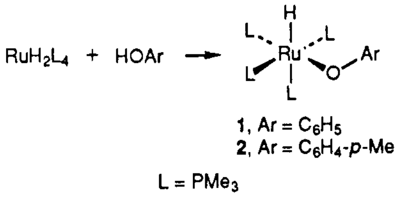

(1)

IR spectra of complexes 1 and 2 show characteristic bands due to ν(Ru–H) vibrations at 1820 and 1828 cm^{-1}, respectively. Table I summarizes NMR data for the complexes. The ^1H NMR spectrum of 1 shows a signal due to the hydride ligand at –8.0 ppm as a doublet of quartets due to ^{31}P–^1H coupling (*J*(PH) = 99 and 28 Hz). The larger *J*(PH) value is assigned to the coupling between the hydride and a trans phosphorus nucleus. The splitting with a coupling constant of 28 Hz is due to the coupling between the hydride and the three cis phosphorus nuclei, which happen to show the same *J*(PH) value. The above coupling pattern of the hydride signal is consistent with the cis structure of the complex, rather than a trans structure, in which four phosphorus atoms would be magnetically equivalent.

The $^{31}P\{^1H\}$ NMR spectrum of 1 shows signals at 16.4, 2.0, and –11.5 ppm, respectively, in a peak area ratio of 1:2:1. The signal at 2.0 ppm is assigned to the two phosphorus nuclei that are situated at mutually trans positions and are magnetically equivalent. Figure 1 compares the observed spectrum at –40 °C in CD_2Cl_2 and a computer-simulated spectrum with an A_2MX spin system. These two spectra agree well with each other. The selective ^1H-decoupled ^{31}P NMR spectrum (irradiated at the signals due to the hydrogens of $P(CH_3)_3$) of 1 shows a splitting of the signal at –11.5 ppm to a doublet with *J*(H–P) = ca. 100 Hz. The *J*(H–P) value thus obtained agrees with the value of 99 Hz obtained from the hydride signal in the ^1H NMR spectrum. These results indicate that the signal at –11.5 ppm is assigned to the PMe_3 ligand trans to the hydride ligand and that the signal at 16.4 ppm is due to the PMe_3 ligand trans to the phenoxide ligand.

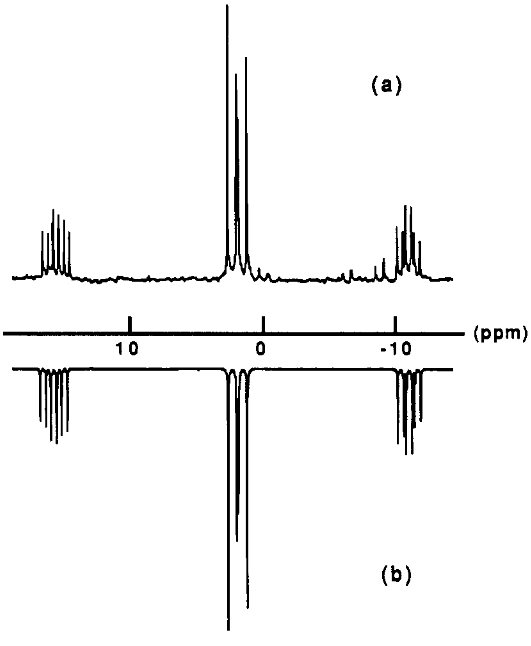

Figure 1. (a) Observed and (b) computer-simulated $^{31}P\{^1H\}$ NMR spectra of *cis*-$RuH(OC_6H_5)(PMe_3)_4$ (1) at –40 °C in CD_2Cl_2.

The $^{13}C\{^1H\}$ NMR spectrum of 1 shows signals due to the phenyl carbon atoms at 171.3, 128.3, 120.2, and 108.9 ppm, which are assigned to the ipso, meta, ortho, and para carbons, respectively, on the basis of a comparison of their positions with those of the corresponding signals in *trans*-$PdMe(OC_6H_5)(PMe_3)_2$.[5a]

The NMR spectra (^1H, ^{13}C, and ^{31}P) of complex 2 are also consistent with the cis structure.

Preparation of *cis*-$RuH(OC_6H_4\text{-}p\text{-}CN)(PMe_3)_4(HOC_6H_4\text{-}p\text{-}CN)$ (3-HOC_6H_4-*p*-CN). The reaction of $RuH_2(PMe_3)_4$ with 2 equiv of *p*-cyanophenol gives a complex formulated as *cis*-$RuH(OC_6H_4\text{-}p\text{-}CN)(PMe_3)_4(HOC_6H_4\text{-}p\text{-}CN)$ (3-HOC_6H_4-*p*-CN).

The ^1H NMR spectrum of 3-HOC_6H_4-*p*-CN shows the hydride signal at –9.3 ppm as a doublet of quartets similar to those of 1 and 2. This ^1H NMR feature as well as the

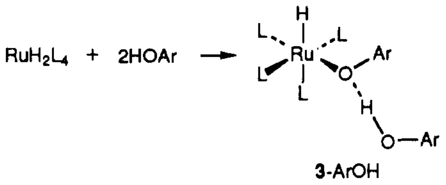

(2)

3-ArOH

L = PMe3, Ar = C6H4-p-CN

$^{31}P\{^1H\}$ NMR spectrum showing an A_2MX pattern clearly indicates a cis structure. The $^{13}C\{^1H\}$ NMR spectrum of 3-HOC_6H_4-*p*-CN at −40 °C shows pairs of signals corresponding to carbon atoms in the *p*-cyanophenoxide ligand and those in the associated *p*-cyanophenol. The ^1H NMR spectrum shows the signal due to the OH hydrogen at 16.3 ppm, which is at considerably lower field than that of free *p*-cyanophenol (ca. 7 ppm in CD_2Cl_2 at room temperature). This peak position is proposed to arise from the O–H···O hydrogen bonding between the *p*-cyanophenoxide ligand and the *p*-cyanophenol in the solution, similarly to the complexes of other transition metals having associated phenols $Rh(OC_6H_4\text{-}p\text{-}Me)(PMe_3)_3(HOC_6H_4\text{-}p\text{-}Me)$,[3] *trans*-$PdH(OPh)(PCy_3)_2(HOPh)$,[4] *trans*-$PdMe(OPh)(PMe_3)_2(HOPh)$,[5a] and *trans*-$PtMe(OPh)(PMe_3)_2(HOPh)$,[5b] which show their hydrogen-bonded OH signals at 14–8 ppm.

Reactions of $RuH_2(PMe_3)_4$ with 2 equiv of phenol or *p*-methylphenol do not give analogous isolable complexes having the phenols associated through O–H···O hydrogen bonding but readily give crystals of complexes 1 and 2 free from the associated phenols. However, the ^1H NMR spectrum of an equimolar mixture of 1 and HOPh (in CD_2Cl_2) shows the OH signal of the phenol at 12.8 ppm, indicating the existence of the association equilibrium of 1 with phenol in the solution to give the phenol adduct 1-PhOH. On the other hand, the reaction of $RuH_2(PMe_3)_4$

$$\underset{1}{RuH(OPh)L_4} + PhOH \rightleftharpoons \underset{1\text{-}PhOH}{RuH(OPh)L_4(HOPh)} \quad (3)$$

with equimolar *p*-cyanophenol gives the complex 3-HOC_6H_4-*p*-CN as crystals in a small amount (<5%). Concentration of the remaining filtrate under vacuum gives an oily product. Although the reaction product is considered to contain $RuH(OC_6H_4\text{-}p\text{-}CN)(PMe_3)_4$ without the associated *p*-cyanophenol in a significant amount, attempts to isolate it by crystallization have not been successful. The exclusive isolation of complexes 1, 2, and 3-HOC_6H_4-*p*-CN, respectively, as crystals from the above reaction mixtures is likely due to a much more facile crystallization of these compounds than for the other complexes present in the reaction mixtures.

Crystal Structure of Complex 2. Single crystals of 2 contain two crystallographically independent molecules that have structures similar to each other. Figure 2 shows the structure of one of these molecules. Tables II and III summarize crystal data and selected bond distances and angles, respectively. In the following discussion on the bond distances we deal with the structural features of the complex shown in Figure 2 for simplicity. Analogous structural features are observed with the other crystallographically independent molecule.

Four phosphorus atoms and one oxygen atom are situated at five coordination sites of a somewhat distorted octahedron. The hydride ligand is considered to occupy the remaining coordination site, although the hydrogen bonded to the ruthenium center is not located in the difference Fourier map. The distance between the ruthenium center and the phosphorus atom trans to the *p*-methylphenoxide ligand (2.234 (3) Å) is shorter than

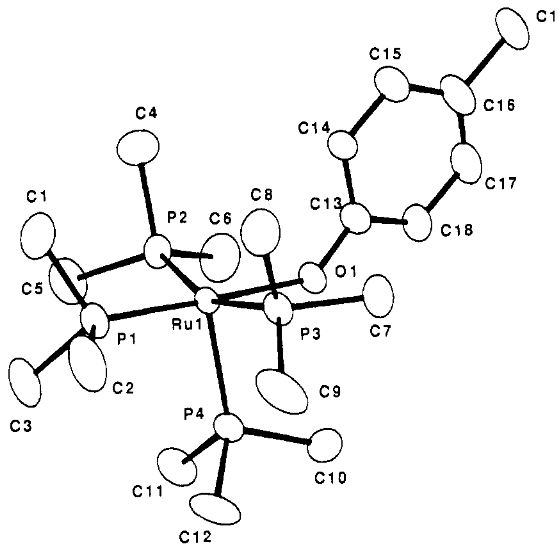

Figure 2. ORTEP drawing of *cis*-$RuH(OC_6H_4\text{-}p\text{-}Me)(PMe_3)_4$ (2), showing 30% probability thermal motion ellipsoids.

Table II. Crystal Data and Details of the Structure Determination of Complex 2

formula	$C_{19}H_{44}OP_4Ru$
mol wt	513.54
cryst syst	monoclinic
space group	$P2_1/a$
a, Å	29.332 (5)
b, Å	13.741 (8)
c, Å	13.568 (3)
β, deg	102.37 (2)
V, Å^3	5341.9
Z	8
μ, cm^{-1}	8.17
$F(000)$	2160
D_{cal}, g cm^{-3}	1.278
cryst size, mm	0.3 × 0.3 × 0.4
2θ range, deg	3.0–50.0
scan rate, deg min^{-1}	4
hkl ranges	$-35 \le h \le 34$, $0 \le k \le 17$, $0 \le l \le 15$
no. of unique rflns	9106
no. of reflns used	6011 ($F_o \ge 3\sigma(F_o)$)
R	0.061
R_w	0.070
weighting scheme[a]	0.062

[a] Parameter q in $[\sigma(F_o)^2 + q^2(F_o)^2]^{-1}$.

Table III. Selected Bond Distances and Angles of the Two Independent Molecules in Complex 2[a]

	Distances (Å)		
Ru1–O1	2.145 (6)	Ru2–O2	2.161 (6)
Ru1–P1	2.234 (3)	Ru2–P5	2.231 (3)
Ru1–P2	2.330 (2)	Ru2–P6	2.331 (2)
Ru1–P3	2.333 (2)	Ru2–P7	2.327 (3)
Ru1–P4	2.376 (2)	Ru2–P8	2.374 (3)
O1–C13	1.31 (1)	O2–C32	1.345 (9)
	Angles (deg)		
O1–Ru1–P1	177.4 (2)	O2–Ru2–P5	177.3 (2)
O1–Ru1–P2	82.4 (2)	O2–Ru2–P6	83.4 (2)
O1–Ru1–P3	85.9 (2)	O2–Ru2–P7	85.4 (2)
O1–Ru1–P4	83.2 (1)	O2–Ru2–P8	82.2 (2)
P1–Ru1–P2	95.1 (1)	P5–Ru2–P6	94.5 (1)
P1–Ru1–P3	96.2 (1)	P5–Ru2–P7	96.2 (1)
P1–Ru1–P4	98.05 (9)	P5–Ru2–P8	99.7 (1)
P2–Ru1–P3	159.89 (9)	P6–Ru2–P7	160.9 (1)
P2–Ru1–P4	97.37 (8)	P6–Ru2–P8	96.8 (1)
P3–Ru1–P4	97.43 (8)	P7–Ru2–P8	96.9 (1)
Ru1–O1–C13	135.9 (5)	Ru2–O2–C32	130.7 (5)

[a] Standard deviations are in parentheses. Distances and angles in the left two columns are those of the molecule in Figure 2. Distances and angles in the right two columns are those of the other crystallographically independent molecule.

those between the ruthenium and the phosphorus atoms P2 and P3 situated at mutually trans positions (2.330 (2) and 2.333 (2) Å) and that between the ruthenium and the phosphorus atom P4 trans to the hydride ligand (2.376 (2) Å). The above results indicate the order of trans influence among these ligands to be as follows: OC_6H_4-*p*-Me < PMe_3 < H.

P–Ru–P angles between the PMe_3 ligands at mutually cis positions, P2, P3, and P4, are considerably larger than 90°, while O–Ru–P angles between the *p*-methylphenoxide and PMe_3 ligands at cis positions are smaller than 90°. These results suggest that steric repulsions between mutually cis PMe_3 ligands are larger than those between the hydride or the p-methylphenoxide ligand and cis PMe_3 ligands. The Ru–O–C bonding is bent so that the steric repulsion between the *p*-methylphenoxide ligand and the PMe_3 ligands is minimized. Ru–O–C angles in the two independent molecules contained in the crystals are 135.9 (5) and 130.7 (5)°, respectively. These angles are larger than the corresponding M–O–C angles of the transition-metal phenoxide complexes *trans*-$PdMe(OPh)(PMe_3)_2$ (127.1 (3)°),[5a] *cis*-$PtMe(OPh)(PMe_3)_2$ (119.8 (9)°),[5b] and $ReO(OPh)(MeC{\equiv}CMe)_2$ (125 (1)°).[8] Bending of M–O–C bonds is commonly observed in late-transition-metal aryloxides and is attributed to arise from π antibonding between the dπ orbital of the metal center and the lone pair of the coordinating oxygen atom.[9] The fact that the C–O–M angle in **2** is larger than those in the above square-planar and tetrahedral complexes suggests weaker π antibonding between the dπ orbital and the *p*-methylphenoxide oxygen in this octahedral complex.[10]

Preparation and NMR Studies of $[RuH_3(PMe_3)_4]OPh$ (4). Reactions of $RuH_2(PPh_3)_4$ with Brønsted acids have been known to give monohydride complexes formulated as $RuHX(PPh_3)_3$ (X = OCOR,[11] SH,[12] SR[13]) accompanied by evolution of dihydrogen and elimination of a PPh_3 molecule. These reactions are considered to proceed through initial protonation of the dihydride complex to give an intermediate complex, having three hydrogen atoms bonded to the ruthenium center, followed by elimination of dihydrogen to give $RuHX(PPh_3)_3$. On the other hand, similar protonation of hydride complexes of group 8 metals has attracted recent attention in relation to the complexes containing dihydrogen[14-21] as the ligand. We have now examined the reaction of $RuH_2(PMe_3)_4$ with phenol at low temperature with NMR spectroscopy in order to determine the structure of the intermediate in reaction 1.

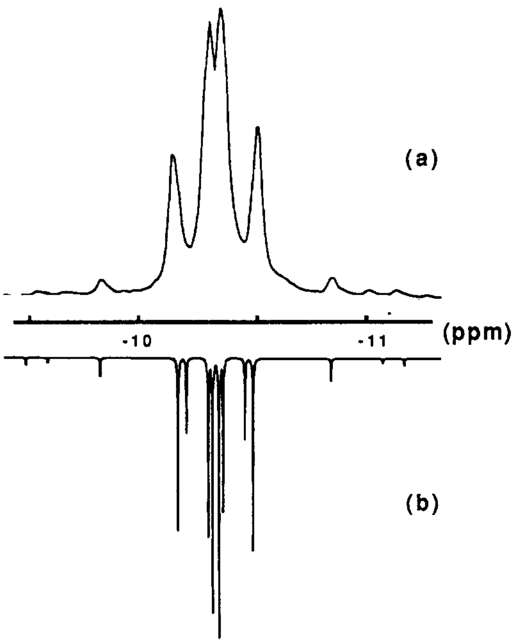

Figure 3. (a) Observed and (b) computer-simulated $^{31}P\{^1H\}$ NMR spectra of $[RuH_3(PMe_3)_4]OPh$ (4), prepared in situ by the reaction of $RuH_2(PMe_3)_4$ with 10 equiv of phenol, at −60 °C in THF-d_8.

The $^{31}P\{^1H\}$ NMR spectrum of a mixture of $RuH_2(PMe_3)_4$ and 10 equiv of phenol in THF-d_8 at −40 °C shows a complicated pattern centered at −10.3 ppm, suggesting the formation of a complex other than $RuH_2(PMe_3)_4$. A computer-simulated spectrum based on an A_2B_2 spin system agrees with the observed signal (Figure 3). The ^1H NMR spectrum of the above reaction mixture shows a broad signal at −8.2 ppm and does not show any other signals assignable to hydrogen atoms bonded to the ruthenium center, indicating the absence of $RuH_2(PMe_3)_4$ and **1**. The peak area ratio of the signal at −8.2 ppm to those of PMe_3 hydrogens in the reaction mixture is ca. 3:36, indicating that three hydrogen atoms are bonded to the ruthenium center in this complex. All these NMR data indicate the formation of the complex $[RuH_3(PMe_3)_4]OPh$ (**4**).

$$RuH_2(PMe_3)_4 + HOPh \rightarrow \underset{\mathbf{4}}{[RuH_3(PMe_3)_4]OPh} \quad (4)$$

In order to confirm the ionic structure of **4**, reactions of $RuH_2(PMe_3)_4$ with other Brønsted acids such as $HOCH(CF_3)_2$ and HBF_4 have been examined. The $^{31}P\{^1H\}$ NMR spectrum of a mixture of $RuH_2(PMe_3)_4$ and $HOCH(CF_3)_2$ (5.2 equiv) shows signals that are in an A_2B_2 pattern. Investigation of a simulated spectrum revealed

---

(8) Erikson, T. K. G.; Bryan, J. C.; Mayer, J. M. *Organometallics* **1988**, *7*, 1930.

(9) Mayer, J. M. *Comments Inorg. Chem.* **1988**, *8*, 125.

(10) The C–O–M angle may be influenced also by packing in the crystal. A significant difference in the angles between the two crystallographically independent molecules is probably due to packing. Conditions of packing around the *p*-methylphenoxide ligands in the crystals were quite different between these two molecules, although remarkable intermolecular interactions were not observed around the *p*-methylphenoxide ligand.

(11) (a) Robinson, S. D.; Uttley, M. F. *J. Chem. Soc., Dalton Trans.* **1973**, 1912. (b) Cole-Hamilton, D. J.; Wilkinson, G. *Nouv. J. Chim.* **1977**, *1*, 141. (c) Osakada, K.; Ikariya, T.; Yoshikawa, S. *J. Organomet. Chem.* **1982**, *231*, 79.

(12) Osakada, K.; Yamamoto, T.; Yamamoto, A. *Inorg. Chim. Acta* **1984**, *90*, L5.

(13) Chaudret, B.; Poilblanc, R. *Inorg. Chim. Acta* **1979**, *34*, L209.

(14) Recent reviews for dihydrogen complexes: (a) Kubas, G. J. *Acc. Chem. Res.* **1988**, *21*, 120. (b) Kubas, G. J. *Comments Inorg. Chem.* **1988**, *7*, 17. (c) Crabtree, R. H.; Hamilton, D. G. *Adv. Organomet. Chem.* **1988**, *28*, 299. (d) Crabtree, R. H. *Acc. Chem. Res.* **1990**, *23*, 95.

(15) (a) Morris, R. H.; Sawyer, J. F.; Shiralian, M.; Zubkowski, J. D. *J. Am. Chem. Soc.* **1985**, *107*, 5581. (b) Bautista, M. T.; Earl, K. A.; Maltby, P. A.; Morris, R. H. *Ibid.* **1988**, *110*, 4056. (c) Bautista, M. T.; Earl, K. A.; Morris, R. H. *Inorg. Chem.* **1988**, *27*, 1124. (d) Bautista, M. T.; Earl, K. A.; Maltby, P. A.; Morris, R. H.; Schweitzer, C. T.; Sella, A. *J. Am. Chem. Soc.* **1988**, *110*, 7031. (e) Ricci, J. S.; Koetzle, T. F.; Bautista, M. T.; Hofstede, T. M.; Morris, R. H.; Sawyer, J. F. *Ibid.* **1989**, *111*, 8823. (f) Cappellani, E. P.; Maltby, P. A.; Morris, R. H.; Schweitzer, C. T.; Steele, M. R. *Inorg. Chem.* **1989**, *28*, 4437.

(16) (a) Arliguie, T.; Chaudret, B.; Morris, R. H.; Sella, A. *Inorg. Chem.* **1988**, *27*, 598. (b) Arliguie, T.; Chaudret, B. *J. Chem. Soc., Chem. Commun.* **1989**, 155. (c) Chaudret, B.; Commenges, G.; Jalon, F.; Otero, A. *Ibid.* **1989**, 210. (d) Arliguie, T.; Border, C.; Chaudret, B.; Devillers, J.; Poilblanc, R. *Organometallics* **1989**, *8*, 1308.

(17) (a) Conroy-Lewis, F. M.; Simpson, S. J. *J. Chem. Soc., Chem. Commun.* **1986**, 506. (b) *Ibid.* **1987**, 1675.

(18) Hampton, C.; Cullen, W. R.; James, B. R. *J. Am. Chem. Soc.* **1988**, *110*, 6918.

(19) Chinn, M. S.; Heinekey, D. M. *J. Am. Chem. Soc.* **1987**, *109*, 5865.

(20) (a) Crabtree, R. H.; Hamilton, D. G. *J. Am. Chem. Soc.* **1986**, *108*, 3124. (b) Hamilton, D. G.; Crabtree, R. H. *Ibid.* **1988**, *110*, 4126.

(21) Tsukahara, T.; Kawano, H.; Ishii, Y.; Takahashi, T.; Saburi, M.; Uchida, Y.; Akutagawa, S. *Chem. Lett.* **1988**, 2055.

that the $\Delta\nu(P_AP_B)$ and $J(P_AP_B)$ values of the signal are quite similar to those of **4**. The ^1H NMR spectrum of the mixture also shows a signal at −7.9 ppm. The reaction of HBF_4 with $RuH_2(PMe_3)_4$ at low temperature also reveals similar NMR spectra, although signals due to some uncharacterized impurities in small amounts are also observed in the $^{31}P\{^1H\}$ NMR spectrum. All of these results indicate the formation of $[RuH_3(PMe_3)_4]OCH(CF_3)_2$ and $[RuH_3(PMe_3)_4]BF_4$ in the above reaction mixtures, respectively. The similarity of the NMR signals of these complexes to the corresponding signals of **4** supports its ionic structure.

The signal due to the OH hydrogens of the phenol contained in the reaction mixture of $RuH_2(PMe_3)_4$ and phenol (Ru:HOPh = 1:10, at −40 °C in THF-d_8) appears at 9.9 ppm, which is at lower field than that of free phenol (ca. 5.8 ppm at room temperature). This can be attributed to association of the phenoxide anion in **4** with phenol in the solution through O–H···O hydrogen bonding:[22,23]

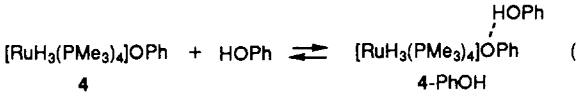

$$\underset{\textbf{4}}{[RuH_3(PMe_3)_4]OPh} + HOPh \rightleftarrows \underset{\textbf{4-PhOH}}{[RuH_3(PMe_3)_4]\overset{HOPh}{O}Ph} \qquad (5)$$

The $^{31}P\{^1H\}$ NMR spectrum of **4**, generated in situ by the reaction of $RuH_2(PMe_3)_4$ with phenol (5 equiv) in THF-d_8, does not change at −40 °C for several hours and for a short time at room temperature. The spectrum measured at −40 °C after the solution is kept at room temperature for 24 h shows that **4** has been completely converted into **1**. These results clearly indicate that reaction 1 proceeds through initial formation of the anionic intermediate $[RuH_3(PMe_3)_4]OAr$ followed by elimination of H_2 to give **1** or **2** or their corresponding phenol adducts:

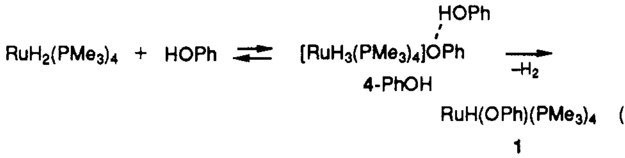

$$RuH_2(PMe_3)_4 + HOPh \rightleftarrows \underset{\textbf{4-PhOH}}{[RuH_3(PMe_3)_4]\overset{HOPh}{O}Ph} \xrightarrow[-H_2]{} \underset{\textbf{1}}{RuH(OPh)(PMe_3)_4} \qquad (6)$$

Raising the temperature of the solution containing $[RuH_3(PMe_3)_4]OCH(CF_3)_2$ to room temperature brings about the appearance of ^{31}P NMR signals at 21.0, −4.8, and −17.0 ppm (A_2MX pattern). These signals can be assigned to *cis*-$RuH(OCH(CF_3)_2)(PMe_3)_4$, although its isolation is not feasible due to its instability.

Examination of changes in the NMR spectra of **4** in acetone-d_6 with time revealed another mode of behavior of the complex in solution. Keeping the solution at room temperature causes a rapid decrease in the peak intensities of the OH and the RuH hydrogens in the ^1H NMR spectrum, although the $^{31}P\{^1H\}$ NMR signals do not undergo any significant change. After 13 min, the intensities of the OH and RuH hydrogen signals in the ^1H NMR spectrum decreased to about 40% of the initial intensities, and these signals disappeared in the room-temperature spectrum after 26 min. An increase in the intensity of the ^1H signal due to the acetone solvent is also observed. A ^2H NMR spectrum measured soon after preparation of the sample at −70 °C shows the presence of a signal at 10.5 ppm, indicating partial deuteration of the OH hydrogen under these conditions. All these results indicate exchange between the OH and RuH hydrogens on the one hand and ^2H of the deuterated acetone solvent on the other. The result of the ^2H NMR measurement of the reaction mixture is interpreted by initial deuteration of the OH hydrogen of the phenol with the deuterated solvent followed by hydrogen exchange between RuH and deuterated phenol. Scheme I shows one of the possible pathways for the deuteration of the hydride ligand and OH hydrogen atoms. The phenoxide anion in **4-PhOH**, formed by reaction of $RuH_2(PMe_3)_4$ with phenol, abstracts a deuterium of acetone-d_6 to give deuterated phenol in a small amount according to eq ii. The DOPh thus formed reacts with $RuH_2(PMe_3)_4$ in the reaction mixture to give the partially deuterated complex **4-PhOH-d_2**. Further deuteration of **4-PhOH-d_2** by repetition of these processes is considered to cause complete deuteration of the RuH hydrogen atoms. Deuteration of all the hydrogen atoms bonded to the ruthenium center indicates the reversibility of the processes (i) and (iii). Recent studies on transition-metal complexes containing dihydrogen[15d,16a,b,17b,20b,24,25] and trihydrogen[16c,d,26] as the ligands have revealed NMR characteristics such as short T_1 values of the hydrogens bonded to the metal center and large $J(HD)$ values of partially deuterated complexes. The T_1 value of the hydride signal in $[RuH_3(PMe_3)_4]OCH(CF_3)_2$ (−40 °C in THF-d_8) is 70 ms at 500 MHz. This value seems to be within the range of nonclassical hydrogen ligated to the metal.[27] The most probable structure of the complex contains a hydride and a dihydrogen ligand that undergo mutual exchange rapidly. Determination of the $J(HD)$ value of $[RuH_2D(PMe_3)_4]OC_6D_5$ (**4-d_6**), prepared by mixing $RuH_2(PMe_3)_4$ with

Scheme I

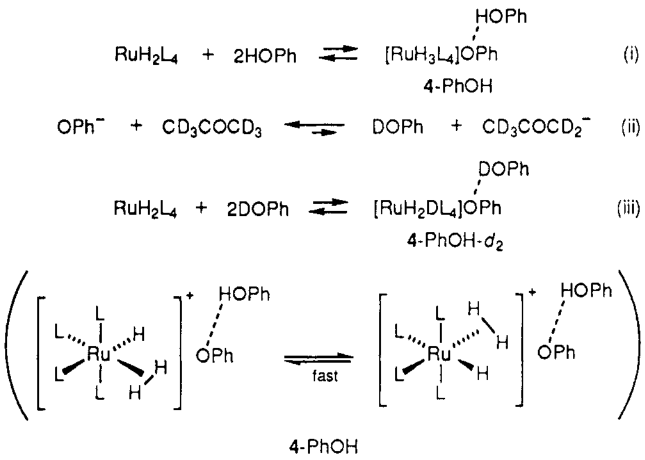

Scheme II

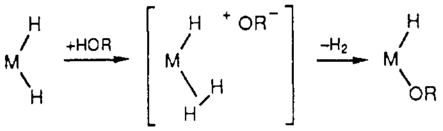

---

[22] Meot-Ner, M.; Sieck, L. W. *J. Am. Chem. Soc.* **1986**, *108*, 7525.

[23] Baer, S.; Stoutland, P. O.; Braumer, J. I. *J. Am. Chem. Soc.* **1989**, *111*, 4097.

[24] (a) Crabtree, R. H.; Lavin, M. *J. Chem. Soc., Chem. Commun.* **1985**, 794. (b) Crabtree, R. H.; Hamilton, D. G. *J. Am. Chem. Soc.* **1986**, *108*, 3124. (c) Crabtree, R. H.; Lavin, M.; Bonneviot, L. *J. Ibid.* **1986**, *108*, 4032. (d) Luo, X.-L.; Crabtree, R. H. *Inorg. Chem.* **1989**, *28*, 3775.

[25] (a) Cotton, F. A.; Luck, R. L. *Inorg. Chem.* **1989**, *28*, 6. (b) *J. Chem. Soc., Chem. Commun.* **1988**, 1277. (c) *J. Am. Chem. Soc.* **1989**, *111*, 5757.

[26] (a) Heinekey, D. M.; Payne, N. G.; Schulte, G. K. *J. Am. Chem. Soc.* **1988**, *110*, 2303. (b) Heinekey, D. M.; Milar, J. M.; Koetzle, T. F.; Payne, N. G.; Zilm, K. W. *Ibid.* **1990**, *112*, 909.

[27] Recently it was reported that classical polyhydride complexes sometimes show relatively short T_1 values.[25] A recent review[14d] has concluded that the minimum T_1 value for a nonclassical complex has never been more than 35 ms at 250 MHz, which is calibrated to be 70 ms at 500 MHz. Although a detailed variable-temperature T_1 measurement is not feasible in the present case due to the temperature-dependent broadening of the signal, the minimum T_1 is considered to be shorter than 70 ms at 500 MHz, which was obtained from measurement at −40 °C.

phenol-d_6 (10 equiv), was not successful due to the broad line width of the hydride signal of 4 and 4-d_6 ($\nu_{1/2} > 50$ Hz).

Conclusions

$RuH_2(PMe_3)_4$ reacts with phenol, *p*-methylphenol, and *p*-cyanophenol smoothly to give complexes with hydride and aryloxide ligands. The reactions involve the intermediate cationic ruthenium complex $[RuH_3(PMe_3)_4]OAr$, which is in equilibrium with $RuH_2(PMe_3)_4$ and HOAr. This ionic complex is stable at −40 °C in solution but is converted into $RuH(OAr)(PMe_3)_4$ gradually at room temperature. $[RuH_3(PMe_3)_4]OCH(CF_3)_2$ similarly prepared by the reaction of $RuH_2(PMe_3)_4$ with $HOCH(CF_3)_2$ at −40 °C has a short T_1 value, indicating the presence of hydrogens bonded to the ruthenium center in a nonclassical coordination manner. The formation of $[RuH_3(PMe_3)_4]^+$ by the reaction of $RuH_2(PMe_3)_4$ with phenol and a fluoro alcohol and subsequent elimination of dihydrogen suggests the reaction sequence shown in Scheme II.[28]

Experimental Section

All the manipulations of the complexes were carried out under argon or in vacuo. $RuH_2(PMe_3)_4$ was prepared according to the literature procedure.[29] Phenol-d_6 was purchased from CEA (Commisariat a l'Énergie Atomique).

Elemental analyses were carried out by Dr. Masako Tanaka of our laboratory with use of a Yanagimoto Type MT-2 CHN autocorder. IR spectra were recorded on a JASCO IR 810 spectrophotometer. NMR spectra were recorded on JEOL FX-100 and GX-500 spectrometers by Dr. Yoshiyuki Nakamura of our laboratory. The T_1 value of the hydride in complex 4 was obtained by the inversion-recovery procedure at 233 K in THF-d_8 (500 MHz).

Preparation of *cis*-$RuH(OC_6H_5)(PMe_3)_4$ (1) and *cis*-$RuH(OC_6H_4$-*p*-$Me)(PMe_3)_4$ (2). To a Schlenk flask containing a mixture of $RuH_2(PMe_3)_4$ (210 mg, 0.51 mmol) and phenol (64 mg, 0.68 mmol) was added THF (2 mL) by trap-to-trap distillation. With continued stirring the mixture was warmed slowly to room temperature and kept for 15 h at that temperature. Evaporation of the solvent followed by addition of acetone (1 mL) to the oily residue gave the complex *cis*-$RuH(OC_6H_5)(PMe_3)_4$ (1) as colorless needles, which were filtered, washed with Et_2O, and dried in vacuo (160 mg, 64%). Anal. Calcd for $C_{18}H_{42}OP_4Ru$: C, 43.3; H, 8.5. Found: C, 43.4; H, 8.5.

cis-$RuH(OC_6H_4$-*p*-$Me)(PMe_3)_4$ (2) was prepared analogously (51%). Anal. Calcd for $C_{19}H_{44}OP_4Ru$: C, 44.4; H, 8.6. Found: C, 43.9; H, 8.8.

Preparation of *cis*-$RuH(OC_6H_4$-*p*-$CN)(PMe_3)_4$-$(HOC_6H_4$-*p*-$CN)$ (3-HOC_6H_4-*p*-CN). To a Schlenk flask containing a mixture of $RuH_2(PMe_3)_4$ (99 mg, 0.24 mmol) and *p*-cyanophenol (59 mg, 0.49 mmol) was added THF (1 mL) by trap-to-trap distillation The temperature of the reaction mixture was gradually raised from −60 °C to room temperature. The colorless solution turned yellow. After the reaction mixture was stirred for 15 h at room temperature, the solvent was removed under reduced pressure. Adding acetone (1.5 mL) to the residue followed by cooling the resulting solution −70 °C gave *cis*-$RuH(OC_6H_4$-*p*-$CN)(PMe_3)(HOC_6H_4$-*p*-CN) (3-HOC_6H_4-*p*-CN) as colorless needles (103 mg, 66%). Anal. Calcd for $C_{26}H_{46}N_2O_2P_4Ru$: C, 48.5; H, 7.2; N, 4.4. Found: C, 48.1; H, 7.4; N, 4.2.

X-ray Crystallography. Crystals of 2 suitable for X-ray crystallography were grown in acetone at −20 °C. Lattice constants were determined by a least-squares calculation of 2θ values of 25 reflections with 19° < 2θ < 22°. Intensities were collected on a Rigaku AFC-5 four-cycle automated diffractometer by using graphite-monochromated Mo Kα radiation (λ = 0.71069 Å).[30] Detailed conditions for the data collection are summarized in Table II. No absorption correction was applied.

Table IV. Atomic Coordinates and Equivalent Isotropic Temperature Factors[a]

atom	*x*	*y*	*z*	B_{eq}, Å^2
Ru1	0.63910 (2)	1.37996 (3)	0.98897 (3)	2.76
Ru2	0.63276 (2)	0.88518 (3)	0.47862 (3)	3.21
P1	0.69785 (9)	1.3849 (2)	0.9118 (2)	4.63
P2	0.64667 (7)	1.2143 (2)	1.0274 (2)	3.94
P3	0.63475 (9)	1.5480 (2)	1.0120 (2)	3.95
P4	0.57662 (9)	1.3667 (2)	0.8411 (2)	4.17
P5	0.6147 (1)	0.8786 (2)	0.6291 (2)	6.46
P6	0.6286 (1)	0.7170 (2)	0.4534 (2)	4.83
P7	0.6189 (1)	1.0512 (2)	0.4521 (2)	5.90
P8	0.7153 (1)	0.8957 (3)	0.5343 (2)	5.72
O1	0.5840 (2)	1.3691 (4)	1.0664 (4)	3.7
O2	0.6480 (2)	0.8860 (5)	0.3304 (4)	4.3
C1	0.7542 (4)	1.3502 (12)	0.9908 (11)	8.8
C2	0.7130 (5)	1.4987 (10)	0.8543 (11)	8.7
C3	0.6980 (4)	1.3058 (9)	0.8028 (10)	7.3
C4	0.6897 (4)	1.1876 (8)	1.1476 (8)	6.5
C5	0.6658 (6)	1.1212 (8)	0.9488 (10)	7.5
C6	0.5945 (4)	1.1552 (7)	1.0482 (11)	7.0
C7	0.5906 (4)	1.5880 (7)	1.0745 (9)	5.9
C8	0.6852 (4)	1.6014 (7)	1.0991 (10)	6.5
C9	0.6238 (7)	1.6378 (8)	0.9101 (9)	9.4
C10	0.5191 (3)	1.3856 (9)	0.8633 (8)	6.0
C11	0.5650 (5)	1.2525 (9)	0.7686 (8)	7.1
C12	0.5742 (5)	1.4502 (11)	0.7344 (8)	8.4
C13	0.5811 (3)	1.3705 (5)	1.1616 (6)	4.0
C14	0.6192 (3)	1.3861 (6)	1.2462 (6)	3.8
C15	0.6133 (4)	1.3891 (7)	1.3450 (7)	4.9
C16	0.5682 (5)	1.3767 (7)	1.3621 (8)	6.0
C17	0.5331 (4)	1.3560 (7)	1.2810 (8)	5.9
C18	0.5392 (4)	1.3519 (7)	1.1846 (8)	5.0
C19	0.5614 (5)	1.3826 (9)	1.4694 (9)	7.8
C20	0.5670 (6)	0.8016 (12)	0.6404 (11)	10.0
C21	0.6601 (7)	0.8305 (18)	0.7401 (11)	14.8
C22	0.5997 (12)	0.9867 (12)	0.6895 (17)	25.7
C23	0.5707 (5)	0.6713 (9)	0.3949 (12)	8.8
C24	0.6479 (5)	0.6270 (7)	0.5525 (10)	6.7
C25	0.6612 (6)	0.6729 (10)	0.3620 (12)	9.2
C26	0.6438 (7)	1.1480 (8)	0.5431 (11)	9.4
C27	0.5581 (9)	1.0845 (13)	0.417 (2)	18.7
C28	0.6328 (10)	1.0999 (10)	0.3417 (13)	15.1
C29	0.7435 (5)	0.931 (2)	0.4375 (12)	17.5
C30	0.7495 (7)	0.7910 (14)	0.590 (2)	14.3
C31	0.7432 (6)	0.9817 (14)	0.6331 (14)	12.1
C32	0.6194 (3)	0.8826 (6)	0.2366 (6)	3.8
C33	0.6424 (3)	0.8824 (6)	0.1552 (6)	4.3
C34	0.6135 (4)	0.8817 (6)	0.0542 (7)	4.8
C35	0.5672 (4)	0.8808 (6)	0.0307 (6)	4.4
C36	0.5458 (3)	0.8825 (8)	0.1112 (7)	5.0
C37	0.5722 (3)	0.8807 (7)	0.2130 (6)	4.6
C38	0.5381 (4)	0.8827 (9)	−0.0783 (8)	6.8

[a] Estimated standard deviations are in parentheses.

Calculations were carried out with the program systems CRYSTAN on a FACOM A-70 computer. The structure was solved by a combination of direct methods (SAPI85) and Fourier techniques. Parameters were refined in full-matrix least-squares calculations by applying anisotropic temperature factors for all the non-hydrogen atoms. Hydrogen atoms in the PMe_3 ligands and phenyl hydrogen atoms in the *p*-methylphenoxide ligand were located at idealized positions with isotropic temperature factors, and their parameters were not refined. The final difference map showed the 10 highest peaks only in the vicinity of the metal centers (within 1.2 Å).

Atomic coordinates of the non-hydrogen atoms are given in Table IV.

---

(28) Two pathways are possible for formation of the intermediate A in Scheme II. One involves the initial formation of a trihydride species, which immediately turns into A. Another involves direct protonation of the hydride of the starting complex to give A. The latter mechanism has also been proposed in the reactions of hydride complexes of tungsten and early transition metals with acid. For example, see: Parkin, G.; Bercaw, J. E. *J. Chem. Soc., Chem. Commun.* **1989**, 255. Our present experimental data are not sufficient to discuss the details of the formation mechanism.

(29) Jones, R. A.; Wilkinson, G.; Colquohoun, I. J.; McFarlane, W.; Galas, A. M. R.; Hursthouse, M. B. *J. Chem. Soc., Dalton Trans.* **1980**, 2480.

(30) Although all the calculations were performed with λ = 0.71069 Å, data collection was carried out with λ = 0.71068 Å.

NMR Study of the Reaction of $RuH_2(PMe_3)_4$ with Brønsted Acids. (a) Reaction with Phenol in THF-d_8. An NMR tube containing $RuH_2(PMe_3)_4$ (47 mg, 0.11 mmol) and phenol (110 mg, 1.1 mmol) was capped with a rubber septum under argon. THF-d_8 (ca. 0.5 mL) was introduced by a syringe. $^{31}P\{^1H\}$ and ^1H NMR spectra of the mixture were measured after keeping it at room temperature for 1 h: $^{31}P\{^1H\}$ NMR (−60 °C, external 85% H_3PO_4) −10.3 ppm (A_2B_2 pattern, $\Delta\nu(P_AP_B) = 32$ Hz, $J(P_AP_B) = 39$ Hz); ^1H NMR (−40 °C) δ 9.9 (O*H*), 7.3–7.0 (C_6H_5), 1.3–1.2 ($P(CH)_3)_3$, −8.2 (Ru*H*).

(b) Reaction with Phenol in Acetone-d_6. After $RuH_2(PMe_3)_4$ (60 mg, 0.15 mmol) and phenol (75 mg, 0.80 mmol) were introduced into an NMR tube equipped with a glass joint, acetone-d_6 (ca. 0.7 mL) was transferred by trap-to-trap distillation. ^1H and ^2H NMR spectra were measured soon after sealing the sample tube: ^1H NMR (−40 °C) δ 12.4 (O*H*), 7.2–6.8 (C_6H_5), 1.5–1.3 ($P(CH_3)_3$), −7.9 (Ru*H*); ^2H NMR (−70 °C) 10.5 ppm (O*D*). The ^1H NMR spectrum after reaction at room temperature for 13 min showed the decrease of peak area of OH and RuH hydrogen signals to ca. 40% of the initial peak areas. These signals disappeared completely after reaction at room temperature for 26 min, although the $^{31}P\{^1H\}$ NMR spectrum showed retention of the same spectroscopic pattern as for 4.

(c) Reaction with 1,1,1,3,3,3-Hexafluoro-2-propanol in Acetone-d_6. After $RuH_2(PMe_3)_4$ (66 mg, 0.16 mmol) and 1,1,1,3,3,3-hexafluoro-2-propanol (140 mg, 0.83 mmol) were introduced into an NMR tube equipped with a glass joint, acetone-d_6 (ca. 0.8 mL) was transferred by trap-to-trap distillation. $^{31}P\{^1H\}$ and ^1H NMR spectra of the reaction mixture were measured soon after sealing the sample tube: $^{31}P\{^1H\}$ NMR (−40 °C, external H_3PO_4) −9.7 ppm (A_2B_2 pattern); ^1H NMR (−40 °C) δ 9.5 (O*H*), 4.7 (C*H*, septet, $J(HF) = 7$ Hz), 1.5–1.4 ($P(CH_3)_3$), −7.9 (Ru*H*). The $^{31}P\{^1H\}$ NMR spectrum after reaction at room temperature for 40 min indicated the decrease of the signal at −9.7 ppm to ca. 75% of the initial peak area. The growth of new signals at 21.0, −4.8, and −17.0 ppm (A_2MX pattern) was observed. After 80 min the signal at −9.7 ppm decreased to ca. 45%. After 24 h all these signals disappeared to give signals of uncharacterized complexes. The isolation of *cis*-$RuH(OCH(CF_3)_2)(PMe_3)_4$ from the reaction mixture as well as its full characterization by NMR spectroscopy was not feasible due to its instability.

(d) Reaction with HBF_4 in Acetone-d_6. An NMR tube containing $RuH_2(PMe_3)_4$ (35 mg, 0.085 mmol) and HBF_4 (48% aqueous solution, 31 mg, 0.17 mmol) was capped with a rubber septum under argon. Acetone-d_6 (ca. 0.7 mL) was introduced by a syringe. $^{31}P\{^1H\}$ and ^1H NMR spectra of the reaction mixture were measured soon after the preparation of the sample: $^{31}P\{^1H\}$ NMR (−40 °C, external H_3PO_4) −8.8 ppm (A_2B_2 pattern); ^1H NMR (−40 °C) δ 11.7 (HBF_4 and H_2O), 1.5–1.4 ($P(CH_3)_3$), −7.9 (Ru*H*). The $^{31}P\{^1H\}$ NMR spectrum after reaction at room temperature for 4 h showed partial decomposition of the above signals (to ca. 50%) and the formation of uncharacterized complexes.

Acknowledgment. This work was financially supported by a Grant-in-Aid for Scientific Research from the Ministry of Education, Science, and Culture (No. 63470079).

Supplementary Material Available: Figures giving the structures of two independent molecules in the crystals and tables of positional parameters of the hydrogen atoms, anisotropic thermal parameters, and bond distances and angles (10 pages); a table of calculated and observed structure factors (31 pages). Ordering information is given on any current masthead page.

Specific Solvatochromism of the Prototypical Olefin Complexes (η^2-TCNE)M(CO)$_5$ (M = Cr, W) Resulting from n and π Donation of Aprotic Solvents toward the π-Acceptor Ligand

Wolfgang Kaim,* Barbara Olbrich-Deussner, and Thomas Roth

Institut für Anorganische Chemie, Universität Stuttgart, Pfaffenwaldring 55, 7000 Stuttgart 80, FRG

Received April 24, 1990

The solvatochromism of the well-separated long-wavelength charge-transfer bands of the title complexes was studied in 36 aprotic solvents and in dichloromethane solutions of durene and hexamethylbenzene. The observed effects cannot be described with one of the conventional solvent parameters that have been successfully used for other transition-metal carbonyl complexes; however, they may be interpreted consistently in terms of strong n- *and* π-donor contributions from the solvents. Within a three-component M–A–D approximation, the π-accepting TCNE (A) interacts strongly with the low-valent metal fragment (M) on one side and weakly with donor solvents (D) on the other side of the molecular plane. A solvent parameter $E_{CT}(\pi)$ is derived, which should describe the (n + π) donor capability of solvents toward an approximately planar π-electron-accepting entity. The differences between the Cr and W series reflect the dipolar contributions to the total solvent effect.

Introduction

The long-known phenomenon of solvatochromism, i.e. the solvent dependence of absorption features and especially of the color of certain compounds,[1,2] has attracted renewed attention recently because of increasing attempts to understand and design electronic structures of potentially light-harvesting and photosensitizing complexes (excited-state tuning).[3] There is also a more general need for reliable solvent parameters that can be correlated with a number of physical properties and with chemical reactivities of the dissolved species.[1,4] Many of the estab-

---

(1) Reichardt, C. *Solvent Effects in Organic Chemistry*; Verlag Chemie: Weinheim, FRG, and New York, 1979; *Solvents and Solvent Effects in Organic Chemistry*; VCH: Weinheim, FRG, 1988.

(2) (a) Saito, H.; Fujita, J.; Saito, K. *Bull. Chem. Soc. Jpn.* **1968**, *41*, 863. (b) Bock, H.; tom Dieck, H. *Angew. Chem., Int. Ed. Engl.* **1969**, *8*, 674. (c) Burgess, J. *J. Organomet. Chem.* **1969**, *19*, 218. (d) Walther, D. *Z. Anorg. Allg. Chem.* **1973**, *396*, 46. (e) Dodsworth, E. S.; Lever, A. B. P. *Chem. Phys. Lett.* **1984**, *112*, 567. (f) Kaim, W.; Ernst, S.; Kohlmann, S. *Chem. Unserer Zeit* **1987**, *21*, 50. (g) Sullivan, B. P. *J. Phys. Chem.* **1989**, *93*, 24.

(3) Kozik, M.; Sutin, N.; Winkler, J. R. *Coord. Chem. Rev.* **1990**, *97*, 1.

(4) (a) Dogonadze, R., Kalman, E., Kornyshev, A. A., Ulstrup, J., Eds.; *The Chemical Physics of Solvation*; Elsevier: Amsterdam, 1985. (b) Cf. the compilation in: Seeber, R.; Piu, P.; Piraino, P.; Zanello, P. *Inorg. Chim. Acta* **1989**, *155*, 27. (c) Catalán, J.; Gômez, J.; Couto, A.; Laynez, J. *J. Am. Chem. Soc.* **1990**, *112*, 1678.